Digital gamma ray tracking algorithms in segmented germanium detectors

C.J.Pearson, J.J.Valiente Dobón, P.H.Regan, P.J.Sellin, E.Morton,
Department of Physics, University of Surrey, Guildford, GU2 7XH, UK.
P.J.Nolan, A.Boston, M.Descovich, J.Thornhill, J.Cresswell,
Department of Physics, University of Liverpool, Liverpool, L69 3BX, UK.
I.Lazarus and J.Simpson
CCLRC Daresbury Laboratory, Warrington, Cheshire WA4 4AD, UK.

Abstract— **A gamma ray tracking algorithm has been implemented and tested, using simulated data, for gamma rays with energies between 0.1 and 2 MeV, and its performance evaluated for a 90 mm long, 60 mm diameter, cylindrical, 36 (6x6) segment detector. The performance of the algorithm in two areas was determined: Compton suppression and Doppler shift correction. It was found that for gamma-rays of energies around 1 MeV, a ratio of photopeak counts to total counts of 70%, using the tracking algorithm could be obtained, with only a 2% reduction in detection efficiency. Approximately 80% of first interaction points could be correctly identified, enabling a good Doppler correction. A detector of the type simulated has recently been delivered, together with a compactPCI digital data acquisition system comprising 36, 12 bit, 40 MHz flash ADCs, and 6 200 MHz DSPs. Some initial data has been recorded using this system, and the performance of the tracking algorithm on this real data is comparable to its performance on simulated data.**

I. Introduction

Over the last twenty years, large volume germanium detectors which form the basis of large gamma-ray arrays have long been cornerstone of nuclear spectroscopy research [1], [2], [3], [4], [5], [6], [7], [8], [9], [10]. The current generation of such detectors have electrically segmented contacts allowing better position resolution to be obtained [11], [12], [13], [14], [15], [16]. It is now possible to divide one or both of the contacts into up to 40 isolated segments, allowing the position within the detector of individual gamma-ray interactions to be determined to an accuracy of better than ~ 5 mm. Such a detector will allow gamma-ray tracking to be performed [13], [14], [15], [17], [18], [19], [20]. The track of gamma-rays entering and scattering within the detector can be determined, enabling the disentangling of multiple gamma-rays entering the detector simultaneously, and, since the original photon interaction is well determined, allows a much more accurate Doppler shift correction [21], [22]. This also enables good imaging of the source, which can have useful medical (and other) applications. A further advantage over previous single element style germanium detectors [23], [24], [25], [26] is that the suppression shield surrounding the detector (which is used to identify gamma rays which Compton scatter out of the detector after depositing only a fraction of their energy) is no longer necessary, as these escaping gamma-rays can be identified from their tracks.

The current state of germanium detector developments allowed the following detector to be obtained, from Eurisys Measures, for this project: a coaxial 60 mm diameter, 90 mm long Germanium detector, with a 6 by 6, 36 way, segmented outer contact. The physical segmentation of such a detector provides a limited position resolution of between 20 and 30 mm, and the finite number of segments limits the interaction multiplicity which can be observed. In order to improve this situation, it is necessary to use digital pulse processing techniques to extract more detailed position and multiplicity information from the shape of the detector pulses. This is in contrast to current analogue pulse processing techniques in which only the pulse amplitude and time are recorded. The electronics and data acquisition, obtained to perform this digital pulse processing, is 36 channels of 12 bit, 40 Mhz flash ADCs, with 6 200 Mhz DSPs in a single compact-PCI crate.

II. Detector Simulations

In order to develop tracking algorithms, a simulation of gamma-rays interacting in the 36 segment detector was prepared. The code EGS4 [27], a standard electron and gamma-ray interaction simulator, was used to carry out the simulations. The source gamma-ray energies and detector arrangement are specified and the simulation provides a list of precise interaction positions and deposited energies.

A gamma-ray energy spectrum resulting from the simulation of gamma-rays from a ^{60}Co source interacting in the segmented detector, is shown in Figure 1. This figure shows the characteristics of the data that are to be improved by tracking. The ratio of photopeak counts to total counts is approximately 1/3 i.e. 1/3 of the gamma-rays interacting in the detector deposit their full energy, while the remaining 2/3 Compton scatter out of the detector and escape. Around 70% of gammas entering the detector interact, the other 30% pass straight through. The absolute photopeak efficiency is therefore calculated to be approximately, around 23%, multiplied by the solid angle covered by the detector (this solid angle is approximately 0.5% of 4π, when the detector is placed 25 cm from the source)

The performance of gamma-ray tracking depends strongly on the interaction position resolution that can be obtained from the detector. Gamma rays interact by transferring their energy to electrons, therefore, the interaction

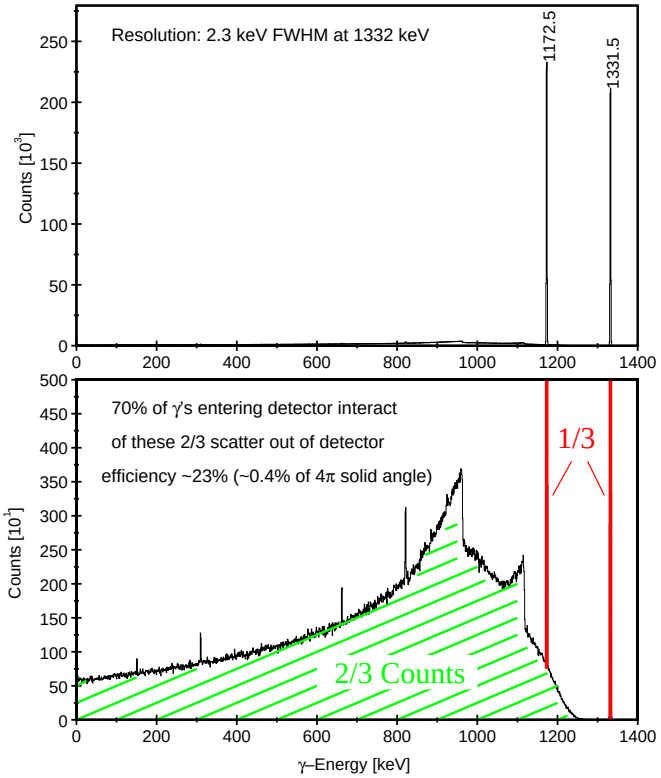

Fig. 1. Gamma-ray energy spectrum resulting from the simulation of gamma rays from a ^{60}Co source interacting in the segmented detector.

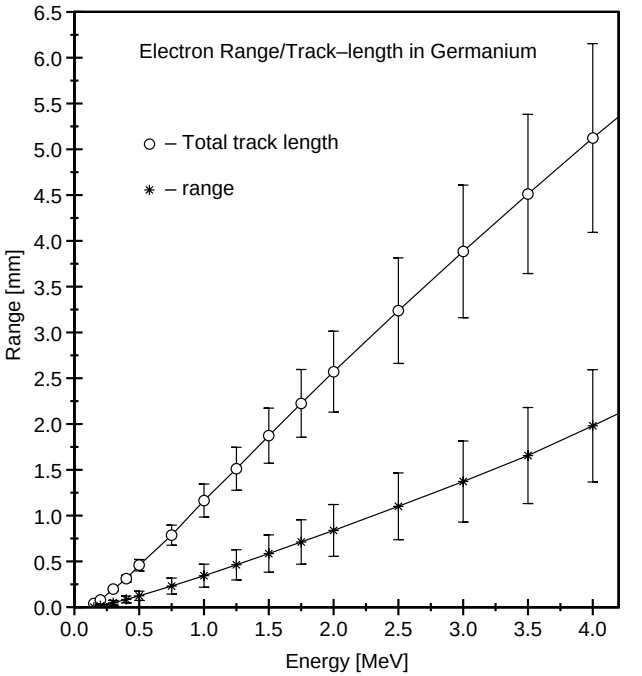

Fig. 2. Simulation of electron range and track length in germanium. The total track length is greater than the range due to scattering.

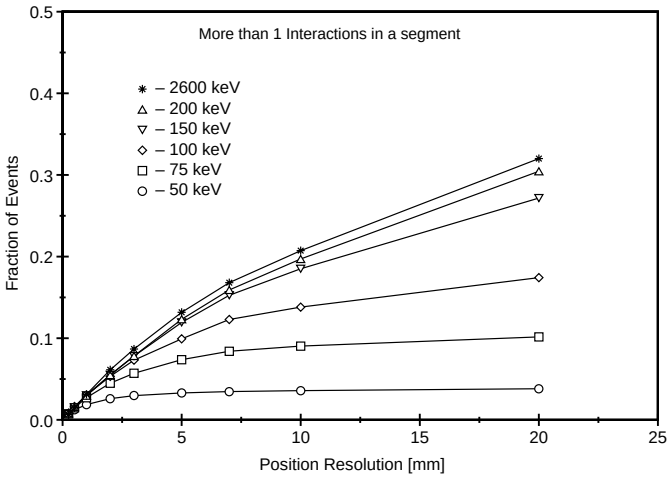

Fig. 3. Simulation of maximum gamma-ray interaction multiplicity per segment, for a range of segment sizes.

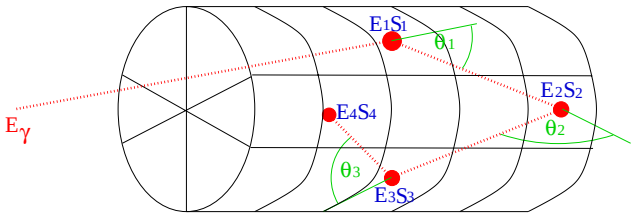

Fig. 4. The data from the detector, or from a simulation, consists of a list of energies and segment numbers.

position resolution is limited by the electron range in germanium. The result of a simulation of electron ranges for various electron energies, (see Figure 2), implies that the range is typically less than than 1 mm for the gamma-ray energies of interest (up to 1.5 MeV).

A further simulation was performed of gamma-rays with energies between 50 keV and 2.5 MeV interacting in the 60 by 90 mm detector, for a range of different position resolutions. The fraction of gamma rays for which more than one interaction occurred in an electronically separated segment was determined. These interactions cannot be separated and will probably not be tracked correctly. The results of this simulation are shown in Figure 3. The fraction of "untrackable" gamma rays varies from around 1/3 with the physical segment size, to about half this with a 5 mm position resolution. This fraction does not vary significantly as a function of energy above 150 keV.

III. Tracking algorithm

The data from the detector (or from a simulation) consists of a list of energies and segment numbers, as shown schematically in Figure 4. It is assumed that the initial gamma-ray energy is the total recorded in the detector. (This assumption will be false if the gamma ray Compton scattered out of the detector). Each possible ordering of the interactions is then tested. This number is not large, as the majority of gamma rays give rise to between 1 and 3 interactions within the volume of the detector. It is also possible to ignore those rare events with many interactions, with little effect on the efficiency. At each point of each of

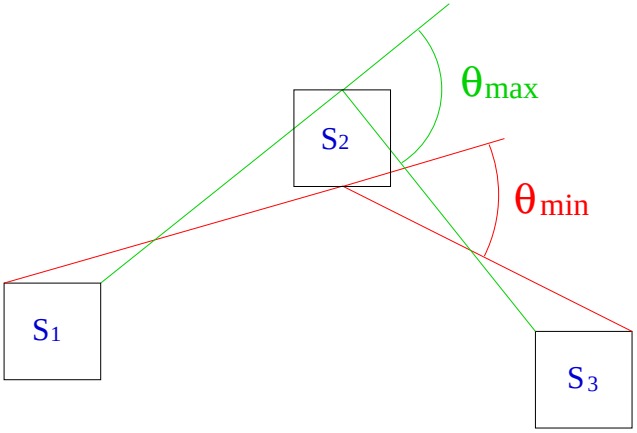

Fig. 5. Finite segment sizes result in a range of possible scattering angles for each Compton scatter.

these tracks the deposited energy is checked for consistency with the possible range of scattering angles at this point in the track (see Figure 5). The deposited energy is related to the scattering angle by the Compton scattering relation,

$$E_{dep} = E_\gamma - \frac{E_\gamma}{1 + E_\gamma / m_0 c(\cos\theta)} \quad (1)$$

This procedure should result in only one interaction ordering being consistent with the data. Alternatively, if there was a Compton escape and the assumption that the whole gamma energy was deposited in the detector is false, then no orderings should be consistent with the data and this event can be rejected.

The finite position resolution available and associated range in scattering angles shown in Figure 5, together with the multiplicity problems described in Section 2, results in a less than ideal performance. As a result, it is possible for several tracks to be consistent with the low-resolution data. In this case, the most probable track is chosen, based on the number of energy dependent mean free paths traveled in the track and also on the variation of differential scattering cross section with scattering angle, using the relation obtained [28] by Klein and Nishina.

IV. Tracking algorithm performance on simulated data

A. Compton suppression

The Compton suppression performance of the algorithm was determined using simulated data. Two sets of results using the tracking algorithm are shown in Figure 6. First, the case with no pulse-shape analysis, where only the physical detector segmentation was used to obtain interaction positions results in a position resolution of between 15 and 30 mm. Secondly, with the segments divided electronically into three in each direction and 5 radially (a division that should be easily achievable) gives a 5 mm resolution.

Those gamma rays giving only a single interaction have to be either included or excluded, as no tracking is possible with only one interaction. Since, in the ^{60}Co case described in the current work, rather high energy gamma-rays (>1

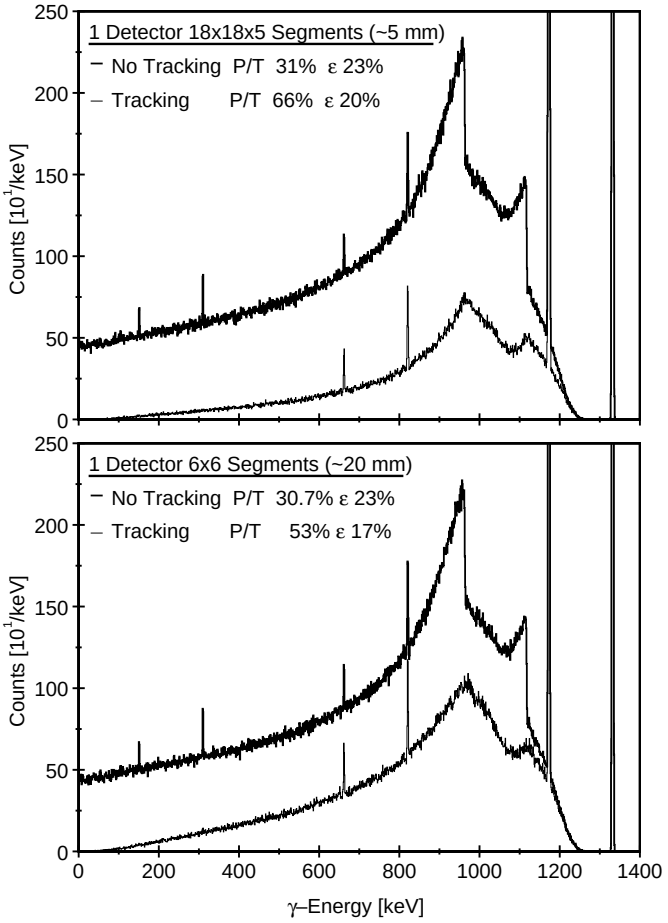

Fig. 6. Compton suppression performance of the tracking algorithm, using simulated ^{60}Co source data.

MeV) are being simulated, single interaction gammas were excluded. The technique of discarding single interaction events is valid for energies above approximately 400 keV but causes the detection efficiency to drop to zero at low energies. To prevent this and retain some efficiency for low energy gamma rays, it will be necessary, at a point based on the total deposited energy, to switch from discarding to accepting single interaction events. This changeover will have to be done smoothly, in order to avoid steps in the resulting spectra. The changeover will also result in an increased Compton background at low energies.

As stated earlier, with no tracking the peak to total ratio is around 1/3 and photo peak efficiency is around 25%. The performance for 5 mm position resolution is that the peak to total ratio is improved from 1/3 to 2/3. This already exceeds the performance of standard BGO shielded detectors whose peak to total ratio is around 50% for detectors of this size. In achieving this, very few full energy events were falsely discarded; the efficiency drops from 23% to 20%. The performance increases rapidly with better position resolution, at 3 mm resolution the peak to total ratio is better than 80%.

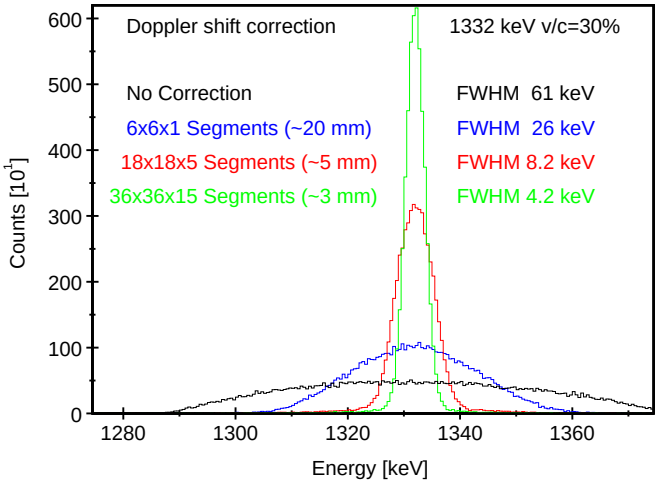

Fig. 7. Doppler shift correction performance of the tracking algorithm using simulated ^{60}Co source data (with v/c=30%).

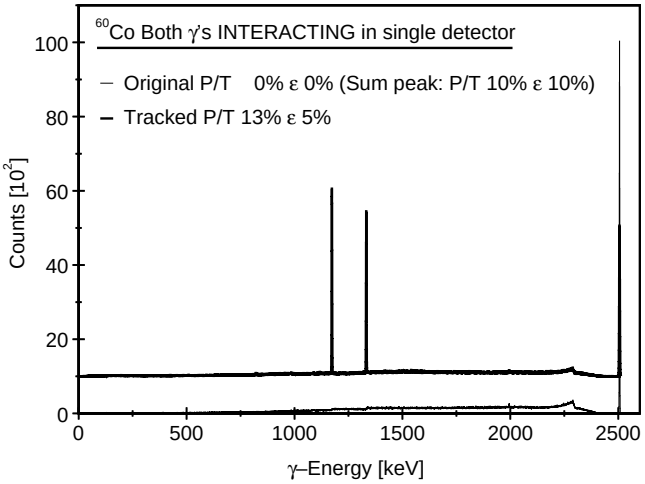

Fig. 8. Tracking algorithm performance for multiple gamma-ray disentanglement (Simulated data). The tracked spectrum is shown offset by 1000 counts.

B. Doppler shift correction

One other measure of the performance of the tracking algorithm, is its ability to enable accurate Doppler shift correction [21], [22]. This depends on identifying the first interaction point, and therefore the angle of the gamma-ray emission from the source. For the energies of interest (up to approximately 1.5 MeV), the tracking algorithm correctly identifies the first interaction point 80 to 90% of the time. Apart from this, the accuracy of the Doppler shift correction is determined by the spatial resolution with which this first interaction position is known.

A source moving with a velocity v, compared to the speed of light c, of v/c=30% was simulated, with the detector positioned at 90 degrees to the source direction at a distance of 25 cm. This angle gives the maximum Doppler broadening for the detected photo-peaks [21]. (Note no variation in the source velocity was included in these simulations). The results of the simulation for a gamma-ray energy of 1332 keV are shown in Figure 7.

With no tracking, the peak is barely visible with a width of over 60 keV. Using only the physical segmentation, this is improved to 26 keV. A more reasonable result of 8 keV is obtained with a 5 mm position resolution. Finally a width of 4 keV, approaching the intrinsic resolution of 2 to 3 keV at this energy, is simulated using a 3 mm position resolution.

C. Additional result for simulated data

A further potential application for the tracking algorithm could be to disentangle multiple gamma rays, simultaneously interacting in a single detector. This is impossible with current detectors. A simulation was set up, again with a ^{60}Co source and the segmented detector. The simulation was set such that *both* the ^{60}Co gamma-rays (1173 and 1332 keV) interacted simultaneously in the detector.

A backtracking scheme was implemented to partition the interactions between separate gamma rays. It is unlikely that any partitioning scheme based on interaction clustering would be successful in such a small volume, where the interactions from a particular gamma-ray are not expected to be well separated from interactions due to other gammas. The backtracking method involved choosing a photoelectric and final Compton scatter pair of interactions. As previously, all possible combinations were tested. Each remaining interaction was then tested for consistency as a possible previous Compton scatter, the test being the scattering angle selection method discussed earlier. Of the partitioning accepted by this selection, that in which the largest number of interactions can be assigned to one gamma-ray was chosen. The process was then repeated until all interactions were assigned.

The results of this simulation are shown in Figure 8. Since both gammas interact, the untracked data has no peaks at 1173 and 1332 keV, only a sum peak at 2505 keV. As a result, the untracked peak to total ratio and efficiency are both zero. The tracking algorithm, using a 5 mm position resolution, can recover the 1173 and 1332 keV gamma-rays from a significant fraction of these events. Figure 8 shows that large peaks at these energies appear in the tracked spectrum.

V. Detector and data acquisition system

A cylindrical 90 mm long, 60 mm diameter, closed-ended coaxial, 36 (6x6) segment, germanium detector is currently being tested. A photograph of the detector, taken soon after delivery in January 2001, is shown in Figure 9. Figure 10 shows a view of the detector with the preamplifier housing removed, and the 36 preamplifier boards in view.

A digital data acquisition system was designed specifically for this detector. This consisted of a compactPCI crate containing a host computer board and 6 200 MHz DSP boards each with 3, dual, 40 MHz, 12 bit flash ADC daughter boards. A photograph of the acquisition system is shown in Figure 11. The system is able to capture digitised pulses from each of the 36 detector segments, triggered using the center contact signal. The ADC sample rate is variable up to a maximum of 40 MHz, with up to 1024

Fig. 9. Photograph of the 6x6 segmented germanium detector.

Fig. 11. Data acquisition system.

Fig. 10. 36 Preamplifier boards in situ in the detector.

sample points, corresponding to 25 μs at the 40 MHz sample rate available per trigger. Currently only 256 samples, 5 μs, are taken as this is thought to give sufficient energy resolution and significantly reduces the data rate.

The system has been running without problems at a trigger rate of 100 per second and will be capable of running much faster than this when some extra pulse processing has been applied to reduce the data rate.

VI. Detector performance

The energy resolution for each of the detector segments was measured for both low energy and high energy gamma-rays using standard analogue electronics with 6 μs shaping. The results, given in Figure 12, show the resolution is approximately 1.8 keV at 122 keV, increasing to 2.5 keV at 1332 keV with small variations between segments.

The rising part of the pulses from the detector segments contain [17] information on interaction positions within the segment. Figure 13 shows the distribution of pulse risetimes for two segments. The risetimes vary between 100 and 250 ns. This figure shows the slightly larger risetimes from interactions in the front, non-coaxial, part of the detector where the electric field is lower than in the rest of the detector.

Further information on interaction positions within a segment can be obtained [18] by observing the induced signals on its neighboring segments, in particular, the location of the neighboring segment with the largest induced signal and the polarity of this signal. The amplitude of induced signals in a segment decreases with increasing distance be-

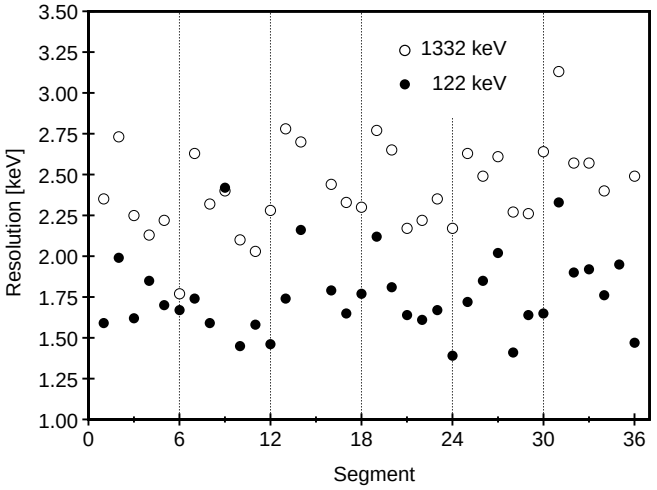

Fig. 12. Measured detector segment energy resolutions at 122 and 1332 keV.

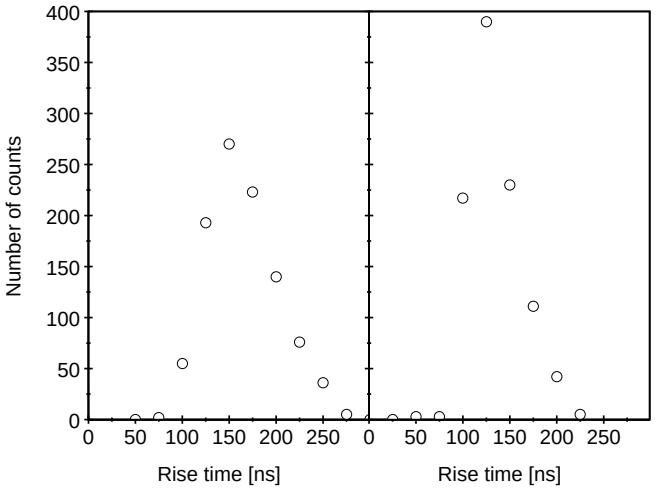

Fig. 13. The diagram to the left shows the distribution of pulse rise times observed in a segment from the front part of the detector. The diagram to the right shows the observed risetime distribution in one of the third row of segments, which are in the coaxial part of the detector.

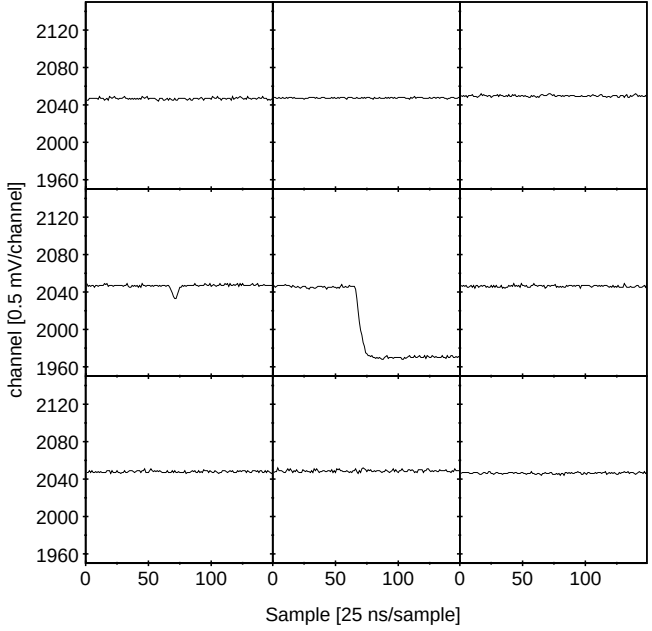

Fig. 14. Digitised segment signals for (center) a segment in which a gamma-ray interaction deposited approximately 100 keV, and signals taken at the same time from the eight surrounding segments showing (center left) an induced signal.

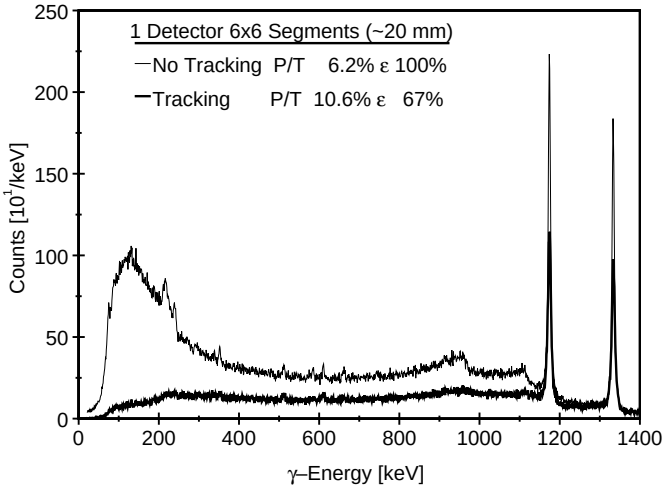

Fig. 15. Results of tracking algorithms applied to ^{60}Co source data taken with the segmented detector and digital data acquisition system.

tween interaction positions and that segment. The sign of induced signals gives information on the radial position of the gamma-ray interactions. Typical digitised segment signals are shown in Figure 14. A signal due to a gamma-ray interaction and also an induced signal on a neighboring segment are shown in this Figure.

VII. Tracking algorithm performance for ^{60}Co source data in the lab

Experimental ^{60}Co source data was taken with the source at a distance of 25 cm from the face of the detector (to allow a direct comparison with the simulated data discussed earlier). The data consists of the 36 digitised signals from the preamplifiers of the detector segments. Each signal has 256 12 bit sample (one sample every 25 ns) covering around 5 μs in total. Approximately 1.25 μs of this time period is before the trigger point, as shown in Figure 14). Initially, simple algorithms were developed to extract interaction energies from the digitised pulses. The process involved fitting the tail of the pulses, 3.5 μs being available to fit. Using this simple technique, an energy resolution of approximately 4 keV was obtained. This resolution was later improved to around 3.5 keV, comparable to that using analogue electronics, using a standard Moving Window Deconvolution (MWD) algorithm [29], [30].

Using the energies obtained above and taking simply the physical segmentation of the EURYSIS detector, the tracking algorithms were applied to the experimental data. The results shown in Figure 15 were obtained. These results are in reasonable agreement with those for the simulated data, although the peak to total ratio for the real data is much worse than that for the simulated data. This is due to

scattering of gamma rays into the detector from surrounding material (such as the detector cryostat). These effects were not included in the simulation. Using the tracking algorithm, the experimental peak to total ratio is doubled compared to the untracked spectrum (6% to 11%) and the efficiency drops to 2/3 its original value.

VIII. Summary

The performance of a tracking algorithm on simulated data of various energies, for both Compton suppression and Doppler shift correction is extremely promising. In addition, the possibility of allowing multiple gamma-rays to enter a single detector simultaneously and to then disentangle them has been demonstrated. The detector and data acquisition system are now complete and working reliably. The performance of the tracking algorithms for the currently available, experimental data appears to be similar to their simulated performance.

Acknowledgments

This work is supported by a Novel Instrumentation grant from EPSRC (UK).

References

[1] J.F. Sharpey-Schafer and J. Simpson Prog. Part. Nucl. Phys. 21 (1988) p293
[2] B. Herskind et al. Nucl. Phys. A447 (1985) p353c
[3] J.P. Martin et al. Nucl. Inst. Meth. A257 (1987) p301
[4] I.Y. Lee Nucl. Phys. A520 (1990) p641c
[5] P.J. Nolan and P.J. Twin, Ann. Rev. Nucl. Part. Sci. 38 (1988) p533
[6] P.J. Nolan et al. Ann. Rev. Nucl. Part. Sci. 45 (1994) p561
[7] C.W.Beausang and J.Simpson, J.Phys. G 22 (1996) 527.
[8] G. Duchene et al. Nucl. Inst. Meth. A432 (1999) p90
[9] P.M. Jones et al. Nucl. Inst. Meth. A357 (1995) p458
[10] J. Eberth et al. Nucl. Inst. Meth. A369 (1996) p135
[11] S.L. Shepherd et al. Nucl. Inst. Meth. A434 (1999) p373
[12] J. Simpson et al. Heavy Ion Physics 11 (2000) p159
[13] M.A. Deleplanque et al. Nucl. Inst. Meth. A430 (1999) p292
[14] G.J. Schmidt et al. Nucl. Instr. Meth. A430 (1999) p69; erratum A434 (1999) p481
[15] K. Vetter et al. Nucl. Instr. and Meth. A452 (2000) p105
[16] W.F.Mueller et al. Nucl. Instr. and Meth. A466 (2001) p492
[17] T. Kröll, I.Peter, T.W.Elze, J.Gerl, T.Happ, M.Kaspar, H.Schaffner, S.Schremmer, R.Schubert, K.Vetter and H.J.Wollersheim, Nucl. Inst. Meth. A371 (1996) p489
[18] T. Kröll and D.Bazzacco, Nucl. Inst. Meth. A463 (2001) p227
[19] J. van der Marel and B. Cederwall Nucl. Inst. Meth. A437 (1999) p538
[20] Th. Kröll and D. Bazzacco Nucl. Instr. Meth. A463 (2001) p227
[21] T. Glasmacher Ann. Rev. Nucl. Part. Sci. 48 (1998) p1
[22] R. Wyss Nucl. Inst. Meth. A256 (1987) p499
[23] P.J.Nolan, D.W.Gifford and P.J.Twin, Nucl. Instr. Meth. A236 (1985) 95.
[24] J.Simpson et al. Nucl. Instr. Meth. A269 (1988) 209.
[25] C.W. Beausang et al. Nucl. Instr. and Meth. A313 (1992) 37
[26] A.M. Baxter et al. Nucl. Instr. and Meth. A317 (1992) 101
[27] W.R.Nelson, H.Hirayama and D.W.O.Rogers, *The EGS4 Code System*, SLAC report No. 265 (1985)
[28] O.Klein and Y.Nishina Z. Phys 52 (1929) p853
[29] A.Georgiev and W.Gast, *Digital Pulse Processing in High Resolution, High Throughput Gamma-ray Spectroscopy*, IEEE Trans. Nuc. Sci, 40 (1993) 770
[30] A.Georgiev et al, *An Analog-to-Digital Conversion Based on a Moving Window Deconvolution*, IEEE Trans. Nuc. Sci, 41 (1994) 1116